Tetrahedron 65 (2009) 9713–9718

Contents lists available at ScienceDirect

Tetrahedron

journal homepage: www.elsevier.com/locate/tet

Tryst with a molecular and supramolecular oddity: an *anti*-Fürst–Plattner epoxide opening product as a designer additive for accessing an elusive polymorph

Goverdhan Mehta *, Saikat Sen

Department of Organic Chemistry, Indian Institute of Science, Bangalore 560 012, India

ARTICLE INFO

Article history:
Received 3 September 2009
Received in revised form
23 September 2009
Accepted 23 September 2009
Available online 26 September 2009

Keywords:
Crystal engineering
Hydrolysis
Hydrogen bonds
Polycyclitols
Polymorphism

ABSTRACT

Additive induced polymorphism of a conformationally locked tetraacetate **3** in presence of its diastereomer **4** is described. The ester **3** was specially crafted on a *trans*-decalin backbone to relegate the O–H···O H-bond donors to the molecular interior and have the peripheral H-bond acceptors in 1,3-syndiaxial relationship. The supramolecular assembly of **3** was destined to evolve along two mutually exclusive pathways, namely one, which employs intermolecular O–H···O H-bonds (*pathway 1*) and the other that sacrifices these for intramolecular O–H···O H-bonds and settles for a crystal packing dictated by weak intermolecular interactions alone (*pathway 2*). Exploiting the similarity between the self-assemblies of **4** and the two recently reported dimorphs of **3**, the ester **3** has been stimulated to follow the elusive non-hierarchical pathway 2 through preferential inhibition of pathway 1. Interestingly, the inhibitor **4** was obtained serendipitously *en route* **3** via an apparent breakdown of Fürst–Plattner rule.

1. Introduction

Intramolecular hydrogen bonds constitute one of the most important non-covalent interactions known in nature in as much as they mould the three-dimensional structure and are therefore linked intimately with the functional aspects of many biological molecules such as proteins and polysachharides.[1] Quite evidently, the structure determining ability of these H-bonds stem from the fact that their formation requires specific molecular conformations that bring the donor and acceptor moieties in close proximity to each other. In small molecules, however, such a conformational constraint often imposes a severe steric repulsion between the functional groups, which cannot often be offset by the stability produced by the intramolecular hydrogen bond. For example, in polyhydroxylated molecules, formation of intramolecular O–H···O hydrogen bonds between hydroxyl groups in 1,3-relationship requires a molecular conformation that allows them to be syn-diaxial to each other.[1a–c] In most examples of naturally occurring polyols, such an orientation of the OH functionalities is energetically unfavorable so that intermolecular O–H···O hydrogen bonds, either to neighboring molecules or solvent, are preferred and observed ubiquitously in the crystal structures of such molecules.[1a–c,2]

Conformationally locked polycyclitols, constructed on a rigid *trans*-decalin carbocyclic backbone **1**, are however required to exhibit an axial rich disposition of the hydroxyl groups, so that the OH functionalities in 1,3-relationship are automatically brought into a favorable geometry for the formation of intramolecular O–H···O hydrogen bonds.[3] Working within this paradigm, which was formulated both logically and on the basis of the observed H-bonding patterns in the crystal structures of several conformationally locked polyols, we were able to demonstrate that intramolecular H-bonding between 1,3-syndiaxial OH groups can even be used as a tool to preordain the positions of the intermolecular O–H···O H-bond donors and acceptors in a specially crafted polycyclitol such as **2**.[3d]

As an extrapolation to our above observations, a study was undertaken to investigate the consequences of disabling the peripheral intermolecular O–H···O H-bond donors, in the form of the secondary hydroxyl groups, in the polycyclitol **2**. To this end, the built-in chemodifferentiation between the hydroxyl groups in **2** was exploited to protect the secondary hydroxyl moieties selectively as their acetate derivatives. Inherent in this substrate design was the expectation that the presence of the two tertiary hydroxyl groups as the sole O–H···O hydrogen bond donors in the polyol **2** would trigger the supramolecular assembly of the tetraacetate **3** of the hexol **2** to evolve along two mutually exclusive pathways. The first follows the hierarchy of the strength of the non-covalent interactions available in **3** and opts for a crystal packing dictated mostly by intermolecular O–H···O H-bonds, employing *albeit* the

* Corresponding author. Tel.: +918023600367; fax: +918023600283.
E-mail address: gm@orgchem.iisc.ernet.in (G. Mehta).

0040-4020/$ – see front matter © 2009 Elsevier Ltd. All rights reserved.
doi:10.1016/j.tet.2009.09.092

lesser accessible tertiary hydroxyl groups (*pathway 1*). The second pathway, on the other hand, relegates the central OH moieties to function merely as intramolecular O–H···O H-bond donors to ester oxygens and settles for a self assembly dictated by weak intermolecular interactions alone (*pathway 2*).[4]

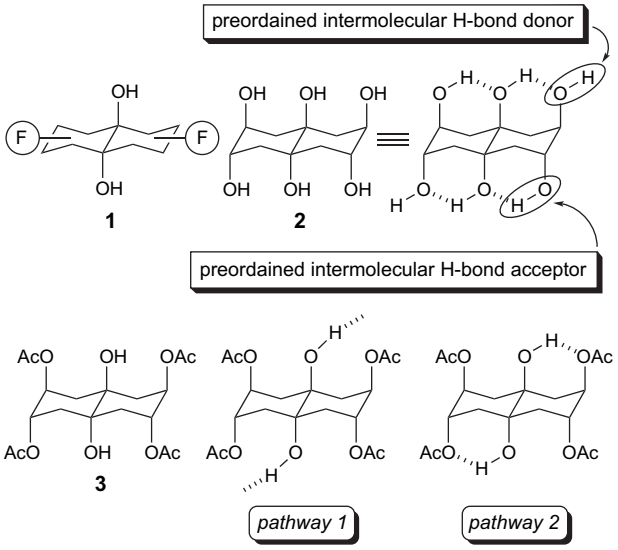

As the first report of this study, we have recently communicated the details of crystal packing and the unusual thermal behavior of the two enantiotropic polymorphs (the α and β forms), obtained upon crystallizing a pure sample of the tetraacetate **3** at two different temperatures.[5] *Albeit* differing in the strength of the intermolecular O–H···O H-bonds, crystal packing in the α and β forms of **3** were essentially similar, both having evolved along pathway 1. Despite altering the conditions and solvent(s) employed, obtaining a polymorphic modification of **3**, which conforms to pathway 2, remained an elusive target.[6] In the present report, we disclose the nature of molecular packing in the third polymorph (the γ form), which has eventually been obtained by inducing **3** to follow pathway 2 through inhibition of pathway 1 by doping the crystallization milieu with a serendipitously encountered isomeric *anti*-Fürst–Plattner tetraacetate **4**.

2. Results and discussion

2.1. Concomitant formation of the isomeric tetraacetates 3 and 4: The serendipitous identification of a competing *anti*-Fürst–Plattner pathway

As reported earlier, the tetraacetate **3** was obtained as the sole compound upon peracetylation of the reaction mixture, obtained after PTSA (*p*-toluenesulfonic acid) catalyzed ring opening of the *anti*-diepoxide **5** in moist dichloromethane.[3d] Evidently, that the *all-trans* hexol **2** would have been the sole stereochemical outcome of the hydrolytic reaction was expected from the well-known Fürst–Plattner rule.[7]

However, in an alternate reaction, it was observed that the diepoxide **5** underwent an extremely slow ring opening (about 48 h) at room temperature in presence of 10% aqueous acetic acid to furnish a reaction mixture, which, upon peracetylation, yielded, in addition to the expected **3**, a minor amount of **4**, evidently the tetraacetate derivative of the hexol **6** (Scheme 1). While quite

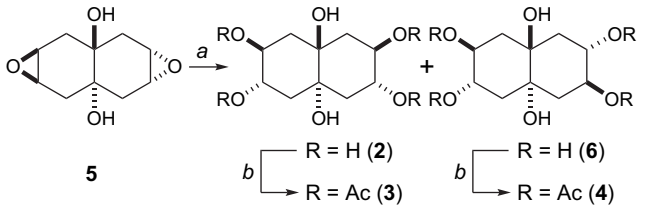

Scheme 1. Reagents and conditions. (a) 10% v/v AcOH (*aq*), RT, 48 h; (b) Ac_2O, DMAP, RT, 10 h [**3**:**4**=9:1; yields over two steps: 44% (**3**) and 5% (**4**)].

intriguing, the concomitant formation of **6**, a diastereomer of **2**, from the diepoxide **5** was best accounted for by invoking a competing *anti*-Fürst–Plattner ring opening[8] in the monoepoxide tetrol intermediate **7** (Scheme 2). Thus, while the major hexol **2** is obtained via a nucleophilic attack of water on **7** at energetically favored position 1, a *trans* diaxial ring opening of the epoxide moiety in **7** from position 2 would engender two new hydroxyl groups in a less favorable twist-boat conformation **8** to yield the minor hexol **6**. Relaxing the carbocyclic skeleton in **8** to a chair conformation in **6** would bring the newly generated OH functionalities to the observed 1,2-diequatorial orientation. Although the *trans-syn-trans-anti-trans* relationship of the oxyfunctionalities in the C_2-symmetric tetraacetate **4** (and thus, its congener **6**) could be discerned from its NMR spectral data, it appeared prudent, given the maverick mode of its formation, to confirm the stereostructure of **4** through single crystal X-ray diffraction studies.

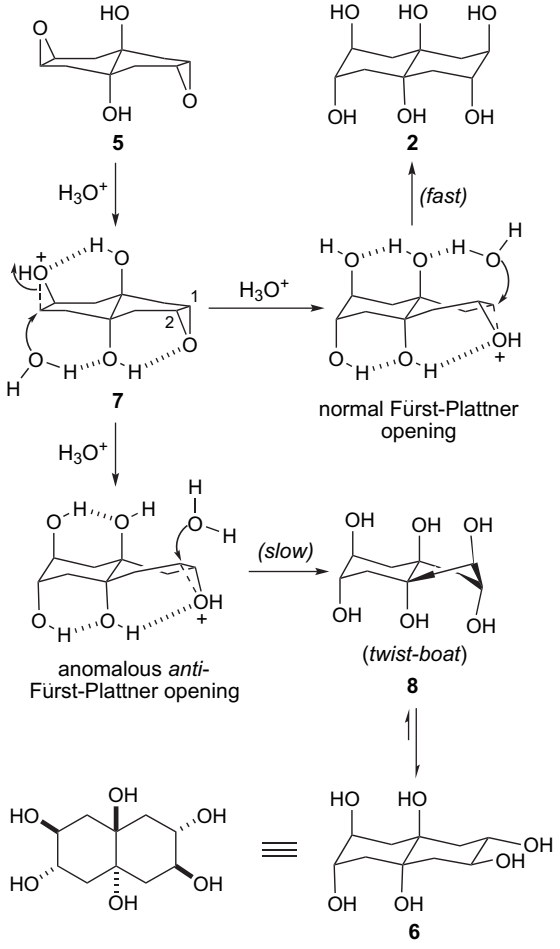

Scheme 2. Mechanism proposed to account for the formation of **6** from **5**.

2.2. Crystal structure of 4 and its isostructurality with the α-form of the isomeric tetraacetate 3

Single crystals of the tetraacetate **4** were obtained as thin plates by slow evaporation of its solution in 2:1 petroleum ether–ethyl acetate mixture at −20 °C. Analysis of the X-ray diffraction data, collected on one such crystal of **4** at both room temperature and 100 K, revealed that the C_2 symmetric tetraacetate packs in the centrosymmetric monoclinic space group $P2_1/c$ (Z=4) and exhibits a striking isostructurality with the α polymorph of **3** (Fig. 1).[5] Indeed, with intermolecular O–H···O hydrogen bonds, linking the tetraacetate molecules into tapes along the *c* axis, and van der Waals forces operating among these molecular tapes translated along the *a* and *b* axes, the pattern of molecular packing in **4** was virtually indistinguishable from that observed in the crystal structures of the α and β polymorphs of **3** (Fig. 2, Table 1).[5] Indeed, this observation led us to believe that the tetraacetate **4** might be employed as a '*tailor-made inhibitor*', which, when present in the crystallization milieu of its diastereomer **3**, would interact preferentially with the precritical nucleii of the α and β forms of **3** through O–H···O hydrogen bonding, thereby arresting pathway 1 and goading the supramolecular assembly in **3** to evolve along the pathway 2.[9]

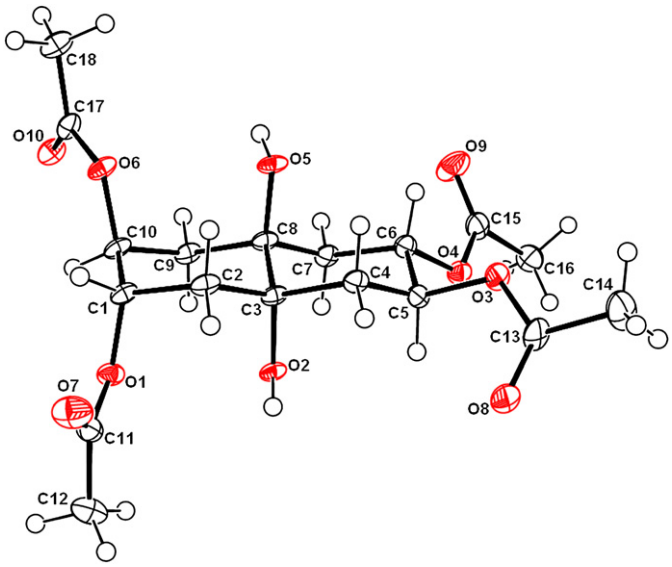

Figure 1. ORTEP diagram of the tetraacetate **4**, with atom numbering scheme for the asymmetric unit. Displacement ellipsoids have been drawn at 50% probability level and H atoms are shown as small spheres of arbitary radii.

2.3. Obtaining the elusive γ-form of the tetraacetate 3

In the light of the preceding argument, crystallization of the tetraacetate **3** in presence of the additive **4** was undertaken. After several crystallization trials with varying solvents and under different ambient conditions, it was observed eventually that a 2:1 M mixture of the tetraacetates **3** and **4**, when crystallized from 1:1 petroleum ether–dichloromethane at −20 °C, furnished a microcrystalline mass, whose PXRD pattern clearly showed the presence of a third polymorph (the γ form) of **3**.[10] The crystallization conditions were optimized, taking this observation as a cue, and finally, slow evaporation of a dilute solution of the tetraacetate mixture in 2:1 petroleum ether-ethyl acetate, containing a trace of methanol, at −20 °C afforded crystals suitable for single crystal X-ray diffraction studies. The crystals, thus obtained, appeared to differ only slightly in their morphology, being both plate-like but one slightly thinner than the other. Hence, having confirmed the presence of

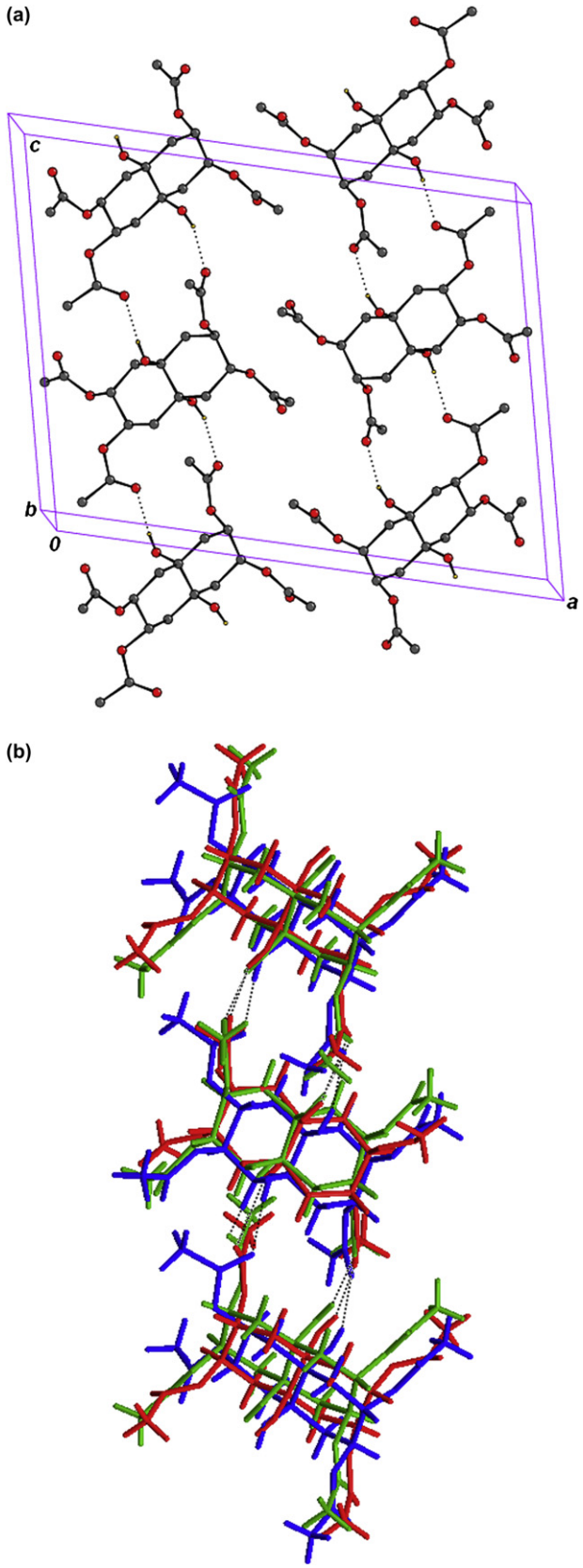

Figure 2. (a) Molecular packing in the tetraacetate **4**. The non-interacting hydrogen atoms have been omitted for clarity; (b) Molecular overlay diagram of the packing in **4** (blue) and, the α (red) and β (green) forms of **3**.

Table 1
Hydrogen bond geometry in the tetraacetate **4**

D–H···A	D–H (Å)	H···A (Å)	D···A (Å)	D–H···A (°)
O2—H2O···O10[a]	0.84	2.05	2.851(3)	160
O5—H5O···O8[b]	0.84	2.00	2.840(3)	174

Symmetry codes.
[a] $x, -y+1/2, z+1/2$.
[b] $x, -y+1/2, z-1/2$.

the γ form of **3** in the admixture through PXRD studies (Fig. 3), extensive cell indexing of individual crystals was undertaken to differentiate the γ form from crystalline **4**.[10]

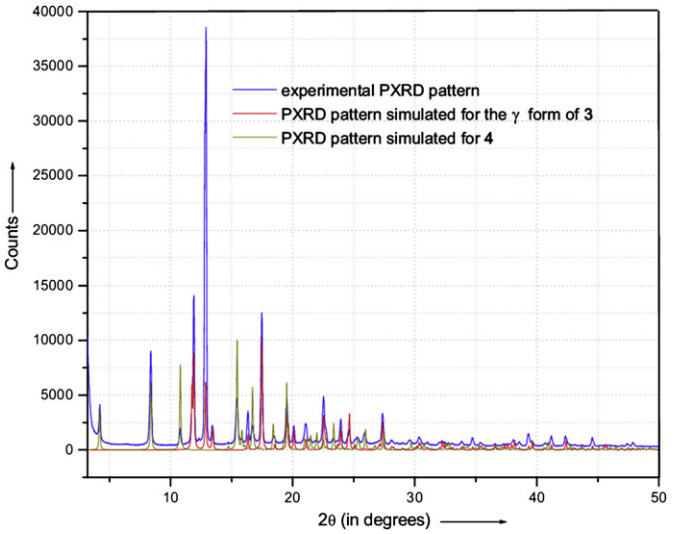

Figure 3. Comparison of the powder X-ray diffraction pattern recorded for the powdered crystals, obtained at −20 °C from a solution of 2:1 mixture of **3** and **4** in 2:1 petroleum ether–ethyl acetate, with those simulated for **4** and the γ form of **3**.

In conformity to our expectations, single crystal X-ray diffraction studies at 100 K revealed that the crystal packing in the γ form of the tetraacetate **3** indeed followed pathway 2. The crystal structure of the γ form was solved in the centrosymmetric monoclinic space group $P2_1/c$ ($Z=2$), with the C_{2h} symmetric tetraacetate molecules occupying the inversion centers at $(0, 0, {}^1/_2)$ and $(0, {}^1/_2, 0)$ (Fig. 4).[11] With the hydroxyl groups engaging themselves in intramolecular O–H···O H-bonding, molecular packing in the γ form was effected via C–H···O hydrogen bonds[12], which connect the tetraacetate molecules to form sheets, essentially parallel to the *ac* plane, and weak van der Waals interactions, which operate between these molecular sheets along the *b* axis (Fig. 5, Table 2).

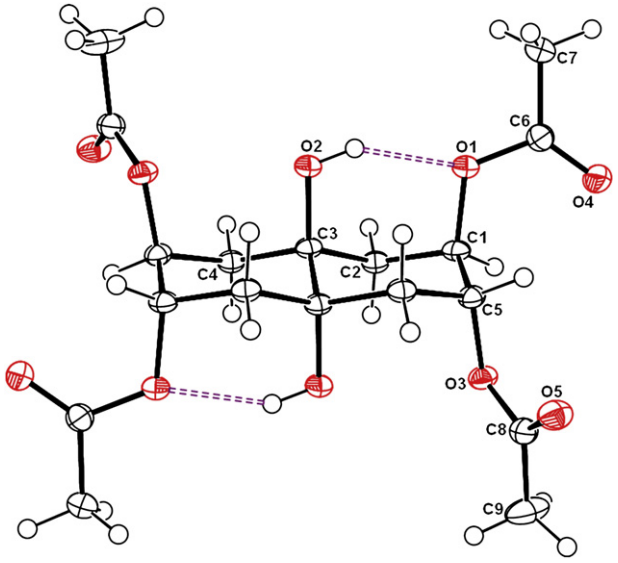

Figure 4. ORTEP diagram of the γ form of the tetraacetate **3**, with atom numbering scheme for the asymmetric unit. Displacement ellipsoids have been drawn at 50% probability level and H atoms are shown as small spheres of arbitary radii. The purple dotted lines indicate the intramolecular O–H···O hydrogen bonds.

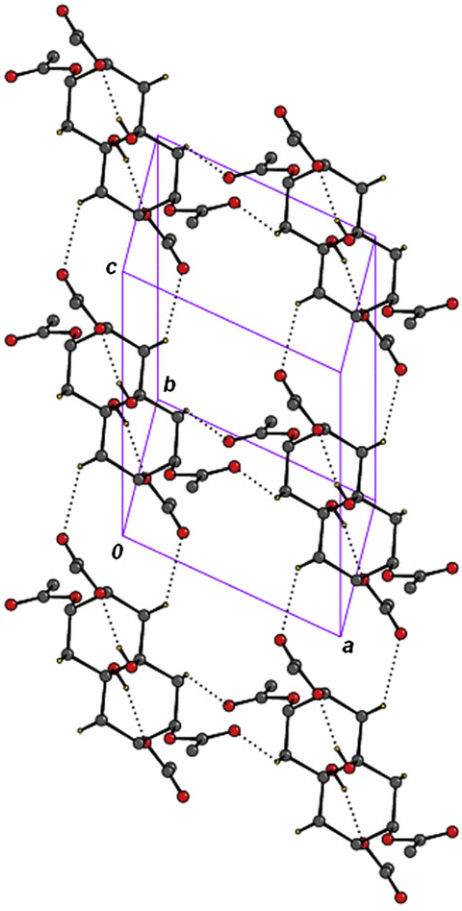

Figure 5. Molecular packing in the γ form of tetraacetate **3**.

Table 2
Hydrogen bond geometry in the γ form of the tetraaceate **3**

D–H···A	D–H (Å)	H···A (Å)	D···A (Å)	D–H···A (°)
O2–H2O···O1[a]	0.84	1.99	2.7360(18)	147
C2–H2B···O4[b]	0.99	2.66	3.404(1)	132
C4–H4A···O5[c]	0.99	2.53	3.321(2)	137

symmetry codes.
[a] x, y, z.
[b] $-x, -y+2, -z$.
[c] $x-1, y, z$.

The successful deployment of **4** as an auxiliary to induce preferential crystallization of the γ polymorph thus vindicated the premise that the otherwise favorable pathway 1 can be blocked by an inhibitor, which is capable of competing with the tetraacetate **3** for the O–H···O hydrogen bonding sites on the surface of the embryonic crystals of **3**. Since the molecular packing in both α and β forms of **3** is effected essentially via the agency of intermolecular O–H···O hydrogen bonds, such an inhibition of crystal growth will be efficacious in stymieing pathway 1. Evidently, the molecules of **4** will interact to a much lesser extent, if

at all, with the precritical nuclei of the γ form, so that its presence in the crystallization milieu will hardly have any effect in the progress of pathway 2 and lead eventually to the isolation of the γ form as the sole polymorph of **3**.

3. Conclusions

As highlighted in a seminal study by Leiserowitz et al., use of '*tailor-made inhibitors*' constitutes a pragmatic approach to control the polymorphic modification during a crystallization process. Such crystallization inhibitors are generally employed as a tool for obtaining metastable polymorphs through preferential inhibition of the stable forms. In the present study, the tetraacetate **4** has been observed to exhibit attributes of a '*tailor-made inhibitor*' and provides access to an elusive polymorphic modification of its diastereomer **3**. It is interesting to note that from a synthetic perspective, the molecular additive **4**, identified serendipitously in the ring opening reaction of the diepoxide **5**, is in itself an oddity, which owes its origin to a minor competing *anti*-Fürst–Plattner pathway in the hydrolysis of **5**. The results of the present endeavor are significant and help to further the understanding of an inadequately researched, yet promising, area of crystal engineering, viz. additive induced polymorphism.[3e,13]

4. Experimental section

4.1. Aqueous acetic acid catalyzed ring opening of the diepoxide 5

A suspension of the diepoxide **5** (100 mg, 0.504 mmol) in 10% aqueous acetic acid solution (5 mL) was stirred at ambient temperature for 48 h. After the completion of the reaction, the volatiles were removed under vacuum and the residue, thus obtained, was put directly for acetylation at room temperature in presence of acetic anhydride (6 mL) and *N*,*N*-dimethyl-4-aminopyridine (271 mg, 2.220 mmol). The reaction takes 10 h to complete as indicated by TLC analysis, after which it was quenched by addition of 4 mL of methanol. Column chromatography carried out on the residue, obtained from the reaction mixture after removal of the volatiles under vacuum, with 50% ethyl acetate/hexane allowed separation of the minor tetraacetate **2** (10 mg, 5% over two steps) from the more polar, major **1** (90 mg, 44% over two steps). Characterization data for **2**: mp 205.8–206.1 °C; IR (neat): $\bar{\nu}$ = 3466, 1733, 1714 cm^{-1};^{1}H NMR (300 MHz, $CDCl_3$): δ=5.26 (dd appearing as a triplet, *J*=5 Hz, 2H), 5.23 (brs, 2H), 2.99 (s, 2H), 2.08 (s, 2H), 2.22 (doublet of $^1/_2$ ABq, *J*=16, 3 Hz, 2H), 2.11 (s, 6H), 2.03 (s, 6H), 1.98–1.90 (m, 4H), 1.78 ($^1/_2$ ABq, *J*=16 Hz, 2H); ^{13}C NMR (100 MHz, $CDCl_3$): δ=170.5 (2C), 168.3 (2C), 73.0 (2C), 70.9 (2C), 69.2 (2C), 37.4 (2C), 32.0 (2C), 21.2 (2C), 21.1 (2C); LRMS (ES, 70 eV) 425 $[M+Na]^+$; HRMS (ES) calcd for $C_{18}H_{26}O_{10}Na$ $[M+Na]^+$:425.1424, found 425.1420.

4.2. Crystallization protocol

4.2.1. Preliminary crystallization trials. All the preliminary crystallization attempts, aimed towards identifying the optimum conditions for obtaining the γ form of **3**, were performed in 5 mL glass sample vials with 10 mg (≈0.02 mmol) of **3** and **4**, present in mole ratios (**3**:**4**) of 10:1, 5:1 and 2:1. With lower proportions of the additive (i.e., **3**:**4**=10:1 and 5:1), the crystallization milieu afforded the best crystals from 1:1 petroleum ether–dichloromethane at −20 °C. As revealed through extensive cell indexing, all the observable single crystals obtained in each case corresponded to the β form of **3**. As already alluded to, a 2:1 M mixture of **3** and **4** afforded, under the same ambient conditions, a microcrystalline mass whose PXRD pattern evidenced the presence of the γ form of **3**.

4.2.2. Obtaining single crystals of the γ form. The tetraacetate **3** (16 mg) and the additive **4** (8 mg) were dissolved in 8 mL of 2:1 petroleum ether-ethyl acetate, containing 0.1% v/v of methanol. This solution was taken in a 10 mL Erlenmeyer flask and allowed to evaporate at −20 °C for 2 weeks when crystals of well-defined morphology and suitable for single crystal X-ray diffraction studies were obtained. Interestingly, endeavors to obtain single crystals of the γ form of **3** in the absence of methanol proved far less fruitful, as the crystals obtained in such cases were either too minute or too ill-defined in their morphology to be employed for crystallographic studies.

4.3. Crystal structure analysis

For data collection at low temperature, a crystal of good quality and reasonable size was mounted in a Lindeman capillary and was cooled slowly from the ambient temperature to 100(2) K at a uniform rate of 40 K/h with an Oxford Cryostream N_2 open-flow cryostat. The temperature of the crystal was then allowed to stabilize for 1 h; the unit-cell parameters were determined repeatedly every 15 min hereafter until the estimated standard deviations in cell dimensions did not vary beyond acceptable limits. Single crystal X-ray diffraction data were collected on a Bruker AXS SMART APEX CCD diffractometer. The X-ray generator was operated at 50 KV and 35 mA using MoK_α radiation. The data was collected with a ω scan width of 0.3°. A total of 606 frames per set were collected using SMART[14] in three different settings of φ (0°, 90° and 180°) keeping the sample to detector distance of 6.062 cm and the 2θ value fixed at −28°. The data were reduced by SAINTPLUS[14]; an empirical absorption correction was applied using the package SADABS[15] and XPREP[16] was used to determine the space group. The crystal structures were

Table 3
Summary of crystal data, data collection, structure solution and refinement details

	3 (α form)[a]	3 (β form)[b]	3 (γ form)[c]	4[d]
Crystal system	Monoclinic	Monoclinic	Monoclinic	Monoclinic
Space group	*C*2/c	*C*2/c	$P2_1$/c	$P2_1$/c
a [Å]	21.433(7)	19.430(4)	8.1946(17)	21.126(5)
b [Å]	5.7126(18)	6.0815(13)	13.627(3)	5.8832(13)
c [Å]	16.720(5)	15.994(3)	9.581(2)	16.533(4)
α [°]	90	90	90	90
β [°]	105.664(5)	91.849(4)	114.764(3)	103.494(4)
γ [°]	90	90	90	90
V [Å^3]	1971.1(11)	1888.9(7)	971.5(4)	1998.2(8)
T [K]	291(2)	100(2)	100(2)	100(2)
Z	4	4	2	4
F (000)	856	856	428	856
ρ_{calcd}[g cm^{-3}]	1.356	1.415	1.376	1.338
μ [mm^{-1}]	0.111	0.116	0.122	0.110
Reflns collected	6929	7047	7509	13,237
l.s.parameters	139	179	130	259
Unique reflns	1800	1853	1959	3659
Observed reflns	1419	1588	1607	2376
R_1 [$I>2\sigma(I)$]	0.0514	0.0343	0.0398	0.0576
wR_2 [$I>2\sigma(I)$]	0.1402	0.0796	0.0938	0.1550
Goodness of fit	1.052	1.034	1.051	0.981

[a] The α form coverts to the β form at −4 °C.[5]

[b] Crystal data for the β form at 291K: monoclinic, *C*2/c, *a*=19.991(5), *b*=6.0024(15), *c*=16.225(4) Å, *β*=91.130(4)°, *V*=1946.5(8) Å^3, *Z*=4, ρ_{calcd}=1.373 g/cm^3, *R*1=0.0405.

[c] Crystal data for the γ form at 291 K: monoclinic, $P2_1$/c, *a*=8.2917(17), *b*=13.742(3), *c*=9.730(3) Å, *β*=114.818(3)°, *V*=1006.4(4) Å^3, *Z*=2, ρ_{calcd}=1.328 g/cm^3, *R*1=0.0447.

[d] Crystal data for the tetraacetate **4** at 291K: monoclinic, $P2_1$/c, *a*=21.603(4), *b*=5.9587(11), *c*=16.596(3) Å, *β*=103.000(3)°, *V*=2081.6(7) Å^3, *Z*=4, ρ_{calcd}=1.284 g/cm^3, *R*1=0.0536.

solved by direct methods using SIR92[16] and refined by full-matrix least-squares methods using SHELXL97.[17] Molecular and packing diagrams were generated using ORTEP32[18], CAMERON[19] and MERCURY[20], respectively. The geometric calculations were done by PARST[21] and PLATON.[22] All hydrogen atoms were initially located in a difference Fourier map. The methine (CH) and methylene (CH_2) H atoms were then placed in geometrically idealized positions and allowed to ride on their parent atoms with C–H distances in the range 0.97–0.98 Å and $U_{iso}(H)=1.2U_{eq}(C)$. The CH_3 and OH hydrogen atoms were constrained to an ideal geometry with C–H distances as 0.96 Å and $U_{iso}(H)=1.5U_{eq}(C)$, and O–H distances fixed at 0.84 Å and $U_{iso}(H)=1.5U_{eq}(O)$. During refinement, each methyl and hydroxyl group was, however, allowed to rotate freely about its C–C or C–O bond, respectively. The details of data collection and refinement are given in Table 3. CCDC 729321 (γ form of tetraacetate **3**) and CCDC 729322 (tetraacetate **4**) contain the supplementary crystallographic data for this paper. These data can be obtained free of charge from The Cambridge Crystallographic Data Centre via www.ccdc.cam.ac.uk/data_request/cif.

Acknowledgements

We thank the Department of Science and Technology (DST), India for the CCD facility at the Indian Institute of Science (IISc), Bangalore. We sincerely acknowledge Prof. K. Venkatesan for his critical comments and helpful advice in preparing the manuscript. GM thanks the Council for Scientific and Industrial Research (CSIR), India for research support and the award of the Bhatnagar Fellowship.

References and notes

1. (a) Jeffrey, G. A. *Acta Cryst., Sect. B: Struct. Sci.* **1990**, *46*, 89–103; (b) Jeffrey, G. A.; Saenger, W. *Hydrogen Bonding in Biological Structures*; Springer: Berlin, 1991; (c) Jeffrey, G. A. *An Introduction to Hydrogen Bonding*; Oxford University Press: Oxford, UK, 1997; (d) Jeffrey, G. A. *Crystallogr. Rev.* **2003**, *9*, 135–176.
2. Mehta, G.; Sen, S.; Dey, S. *Acta Crystallogr., Sect. E: Struct. Rep. Online* **2005**, *61*, o920–o922.
3. (a) Mehta, G.; Sen, S.; Venkatesan, K. *CrystEngComm.* **2005**, *7*, 398–401; (b) Mehta, G.; Sen, S.; Ramesh, S. S. *CrystEngComm.* **2005**, *7*, 563–568; (c) Mehta, G.; Sen, S. *CrystEngComm.* **2005**, *7*, 656–663; (d) Mehta, G.; Sen, S.; Ramesh, S. S. *Eur. J. Org. Chem.* **2007**, 423–436; (e) Mehta, G.; Sen, S.; Venkatesan, K. *CrystEngComm.* **2007**, *9*, 144–151; (f) Mehta, G.; Sen, S. *Eur. J. Org. Chem.* **2009**, 123–131.
4. Over the recent years, a lot of attention has been focused on analyzing, through experimental, theoretical and statistical techniques, the influence that competition between intra- and intermolecular hydrogen bonding might have on the physical and chemical behavior of molecules in gas, liquid or solid phase. Indeed, this subtle interplay goes a long way in determining a number of molecular properties such as the preferred conformation, solubility, acidity and electrochemical behaviour. For recent reports, see: (a) Garcia-Cuellar, A.; Ghonasgi, D.; Chapman, W. G. *Fluid Phase Equilib.* **1996**, *116*, 275–281; (b) Furlani, T. R.; Garvey, J. F. *Mol. Phys.* **1997**, *92*, 449–461; (c) Bilton, C.; Allen, F. H.; Shields, G. P.; Howard, J. A. K. *Acta Cryst., Sect. B: Struct. Sci.* **2000**, *56*, 849–856; (d) Sagadeev, E. V.; Safina, Y. G.; Cherkasov, R. A. *Russ. J. Org. Chem.* **2004**, *40*, 940–945; (e) Baudron, S. A.; Avarvari, N.; Canadell, E.; Auban–Senzier, P.; Batail, P. *Chem.— Eur. J.* **2004**, *10*, 4498–4511; (f) Kooijman, E. E.; Carter, K. M.; van Laar, E. G.; Chupin, V.; Burger, K. N. J.; de Kruijff, B. *Biochemistry* **2005**, *44*, 17007–17015; (g) Infantes, L.; Motherwell, W. D. S. *Z. Kristallogr.* **2005**, *220*, 333–339; (h) Borho, N.; Suhm, M. A.; Le Barbu–Debus, K.; Zehnacker, A. *Phys. Chem. Chem. Phys.* **2006**, *8*, 4449–4460.
5. Mehta, G.; Sen, S. *Chem. Commun.* **2009**, doi:10.1039/b905651c
6. (a) Threlfall, T. L. *Analyst* **1995**, *120*, 2435–2460; (b) Dunitz, J. D.; Bernstein, J. *Acc. Chem. Res.* **1995**, *28*, 193–200; (c) Bernstein, J. *Polymorphism in Molecular Crystals*; Oxford University Press: New York, NY, 2002; (d) also see the special issue on polymorphism in *Cryst. Growth Des.* **2004**, *4*, 1085–1444.
7. (a) Fürst, A.; Plattner, P. A. *Helv. Chim. Acta* **1949**, *32*, 275–283; (b) Fürst, A.; Plattner, P. A. *Abstr. Papers Int. Congr. Pure Appl. Chem., 12th*, New York, NY, 1951; 409.
8. For examples of *anti*-Fürst–Plattner opening of epoxides, see: (a) Barton, D. H. R.; Lewis, D. A.; McGhie, J. F. *J. Chem. Soc.* **1957**, 2907–2915; (b) Leffingwell, J. C.; Royals, E. E. *Tetrahedron Lett.* **1965**, *6*, 3829–3837; (c) Glotter, E.; Greenfield, S.; Lavie, D. *Tetrahedron Lett.* **1967**, *8*, 5261–5263; (d) Lunnon, M. W.; MacMillan, J. *J. Chem. Soc., Perkin Trans. 1* **1977**, 2317–2324; (e) Hashimoto, H.; Araki, K.; Yoshimura, J. *Bull. Chem. Soc. Jpn.* **1981**, *54*, 3015–3019; (f) Sudha, R.; Narasimhan, K. M.; Saraswathy, V. G.; Sankararaman, S. *J. Org. Chem.* **1996**, *61*, 1877–1879.
9. For references on the control of crystal polymorphism via the use of tailor-made nucleation inhibitors, see: (a) Staab, E.; Addadi, L.; Leiserowitz, L.; Lahav, M. *Adv. Mater.* **1990**, *2*, 40–43; (b) Weissbuch, I.; Addadi, L.; Lahav, M.; Leiserowitz, L. *Science* **1991**, *253*, 637–645; (c) Weissbuch, I.; Leiserowitz, L.; Lahav, M. *Adv. Mater.* **1994**, *6*, 952–956; (d) Weissbuch, I.; Popovitz–Biro, R.; Lahav, M.; Leiserowitz, L. *Acta Cryst., Sect. B: Struct. Sci.* **1995**, *51*, 115–148; (e) Davey, R. J.; Blagden, N.; Potts, G. D.; Docherty, R. *J. Am. Chem. Soc.* **1997**, *119*, 1767–1772; (f) Weissbuch, I.; Lahav, M.; Leiserowitz, L. In *Advances in Crystal Growth Research*; Sato, K., Furukawa, Y., Nakajima, K., Eds.; Elsevier Science B.V: Amsterdam, 2001; pp 381–400; (g) Torbeev, V. Y.; Shavit, E.; Weissbuch, I.; Leiserowitz, L.; Lahav, M. *Cryst. Growth Des.* **2005**, *5*, 2190–2196; (h) van Enckevort, W. J. P.; Los, J. H. *J. Phys. Chem. C* **2008**, *112*, 6380–6389; (i) Murali, C.; Shashidhar, M. S.; Gonnade, R. G.; Bhadbhade, M. M. *Chem.—Eur. J.* **2009**, *15*, 261–269.
10. Powder X-ray diffraction data was collected using CuK_α radiation on a Philips PANalytical X'Pert PRO MPD diffractometer, operating at 40 kV and 30 mA.
11. Molecules, possessing a center of symmetry, usually crystallize in centrosymmetric space groups and tend to occupy a crystallographic inversion center; see Brock, C. P.; Dunitz, J. D. *Chem. Mater.* **1994**, *6*, 1118–1127.
12. Desiraju, G. R.; Steiner, T. *The Weak Hydrogen Bond in Structural Chemistry and Biology*; Oxford University Press: Oxford, UK, 1999.
13. For recent reports on additive induced polymorphism, see: (a) Thallapally, P. K.; Jetti, R. K. R.; Katz, A. K.; Carrell, H. L.; Singh, K.; Lahiri, K.; Kotha, S.; Boese, R.; Desiraju, G. R. *Angew. Chem.* **2004**, *116*, 1169–1175; *Angew. Chem. Int. Ed.* **2004**, *43*, 1149–1155; (b) Lee, E. H.; Byrn, S. R.; Carvajal, M. T. *Pharm. Res.* **2006**, *23*, 2375–2380; (c) Lee, E. H.; Boerrigter, S. X. M.; Rumondor, A. C. F.; Chamarthy, S. P.; Byrn, S. R. *Cryst. Growth Des.* **2008**, *8*, 91–97; (d) Kirchner, M. T.; Blaeser, D.; Boese, R.; Desiraju, G. R. *CrystEngComm* **2009**, *11*, 229–231.
14. Bruker. *SMART (Version 6.028), SAINT (Version 6.02), XPREP*; Bruker AXS: Madison, Wisconsin, USA, 1998.
15. Sheldrick, G. M. *SADABS*; University of Göttingen: Germany, 1996.
16. Altomare, A.; Cascarano, G.; Giacovazzo, C.; Guagliardi, A.; Burla, M. C.; Polidori, G.; Camalli, M. *J. Appl. Cryst.* **1994**, *27*, 435.
17. Sheldrick, G. M. *SHELXL97*; University of Göttingen: Germany, 1997.
18. Farrugia, L. J. *J. Appl. Crystallogr.* **1997**, *30*, 565.
19. Watkin, D. M.; Pearce, L.; Prout, C. K. *CAMERON – A Molecular Graphics Package.* Chemical Crystallography Laboratory; University of Oxford: England, 1993.
20. (a) Bruno, I. J.; Cole, J. C.; Edgington, P. R.; Kessler, M. K.; Macrae, C. F.; McCabe, P.; Pearson, J.; Taylor, R. *Acta Crystallogr., Sect. B.* **2002**, *58*, 389–397; (b) Macrae, C. F.; Edgington, P. R.; McCabe, P.; Pidcock, E.; Shields, G. P.; Taylor, R.; Towler, M.; van de Streek, J. *J. Appl. Cryst.* **2006**, *39*, 453.
21. Nardelli, M. *J. Appl. Cryst.* **1995**, *28*, 659.
22. Spek, A. L. *J. Appl. Cryst.* **2003**, *36*, 7.